Supporting Information

Multi-layer hetero-junction anodes for saline wastewater treatment: Design strategies and reactive species generation mechanisms

Yang Yang, Jieun Shin, Justin T. Jasper, Michael R. Hoffmann*

Linde + Robinson Laboratories

California Institute of Technology

Pasadena, California 91125, United States.

*Corresponding author: Email: mrh@caltech.edu

This 18-page file contains ten figures, two tables and one text.

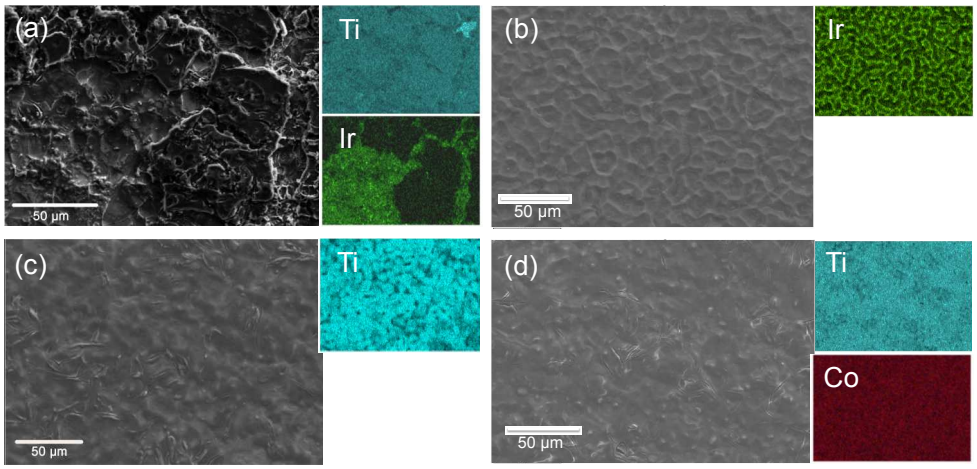

Figure S1. SEM images and EDS elemental mapping of (a) Ti/Ir prepared by brush coating method. (b)Ir, (c) Ti/Ir, and (d) CoTi/Ir anodes prepared by spray-pyrolysis method.

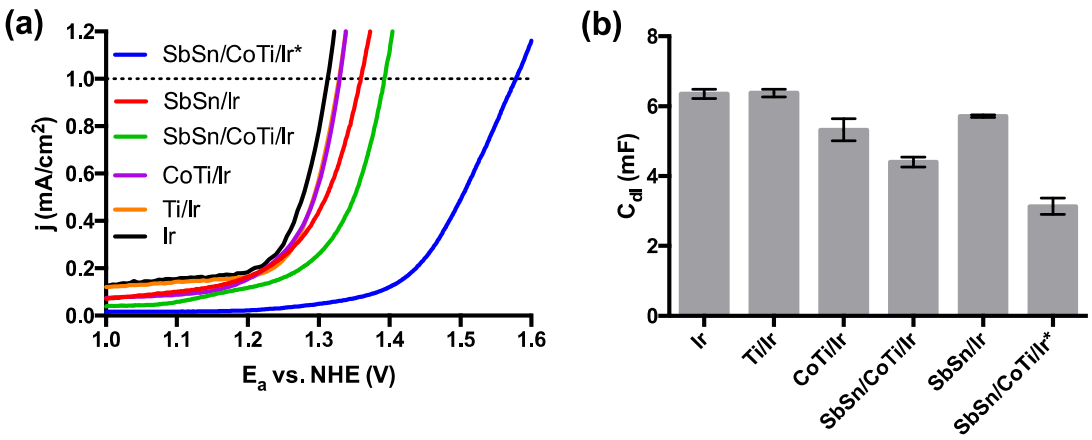

Figure S2. Linear sweeping voltammetries in (a) 30 mM NaCl. (b) Double layer capacities (C_{dl}) measured in 30 mM Na_2SO_4 solution. C_{dl} is reported to be positively correlated with the electrochemically active surface area of OER.[1]

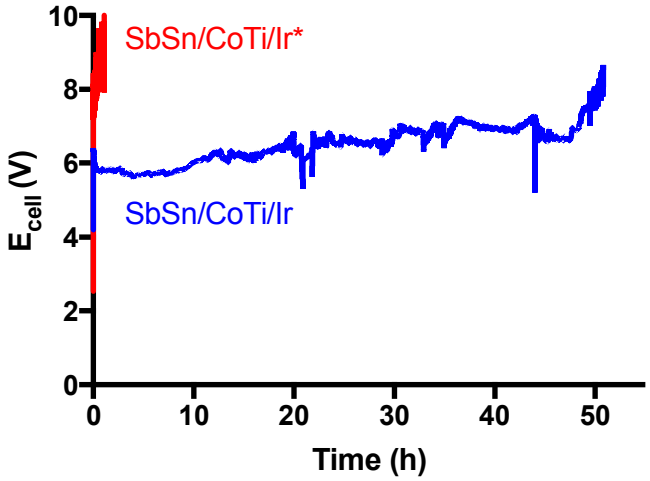

Figure S3. Accelerated lifetime tests (ALT) conducted at a current density of 1.2 A/cm^2 in 1 M $NaClO_4$.

In ALT test, electrode samples with a surface area of 0.25 cm^2 were subjected to 300 mA current, resulting in a high current density of 1.2 A/cm^2. The idea of ALT is to test electrodes under a harsh galvanostatic condition to accelerate the dissolution or detachment of the electroactive layer. Deactivation will be reflected by a sharp increase of cell voltage (E_{cell}). The electrode is considered to be deactivated when the cell voltage reaches 9 V because above this voltage the Ti metal base will be corroded. On the basis of lifetimes (t_{Acc}) observed from ALT at high current (I_{Acc} = 1.2 A/cm^2), the actual lifetime (t) at operational current (I) can be estimated by the empirical equation[2, 3]

$$t = \frac{I_{ac}^{1.7} t_{ac}}{I^{1.7}}$$

The t_{ac} of SbSn/CoTi/Ir* and SbSn/CoTi/Ir is 0.5 and 52 h, which gives the lifetime as 360 h and 37,507 h (ca. 4.3 years) at 25 mA/cm^2.

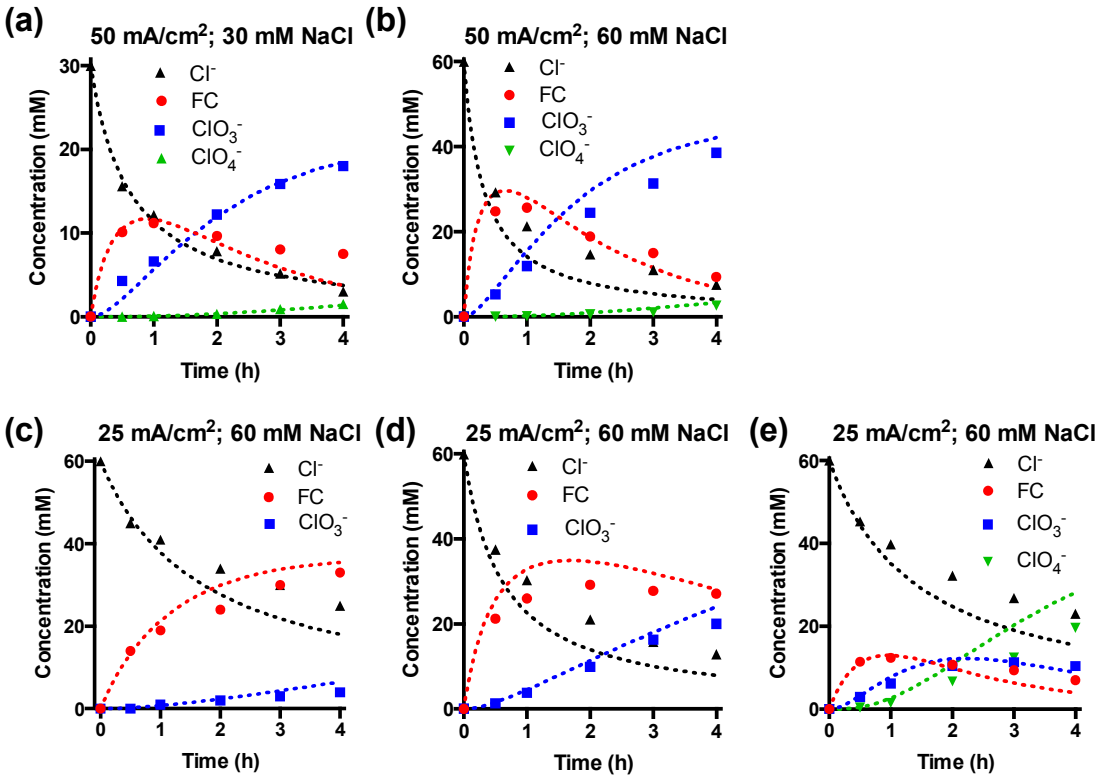

Figure S4. Electrolysis of (a) 30 and (b) 60 mM NaCl with SbSn/CoTi/Ir anode at 50 mA/cm^2. Electrolysis of 60 mM NaCl at 25 mA/cm^2 using the (c) CoTi/Ir, (d) SbSn/CoTi/Ir, and (e) SbSn/CoTi/Ir* anodes. Symbols represent the experimental data. Dashed lines represent the predicted modeled results, except for those of Figure S4d represent model fitting results.

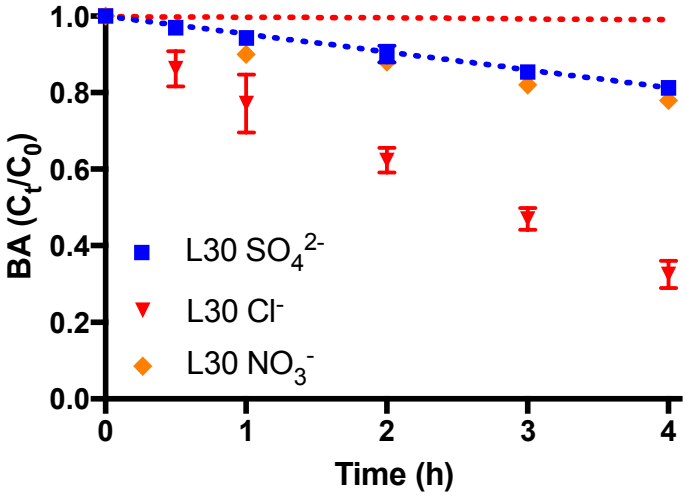

Figure S5. Experimental (dot) and model predicted (dot line) data for BA degradation using the SbSn/CoTi/Ir* anode in 30 mM Na_2SO_4, $NaNO_3$, and NaCl electrolyte at 25 mA/cm^2. BA degradation in 30 mM NaCl was simulated by kinetic model excluding the one-electron oxidation of Cl^- to $Cl\cdot$ (rxn 2 in Table S2). The model predicts that BA was barely degraded in the presence of Cl^-, which is significantly different from experimental results

.

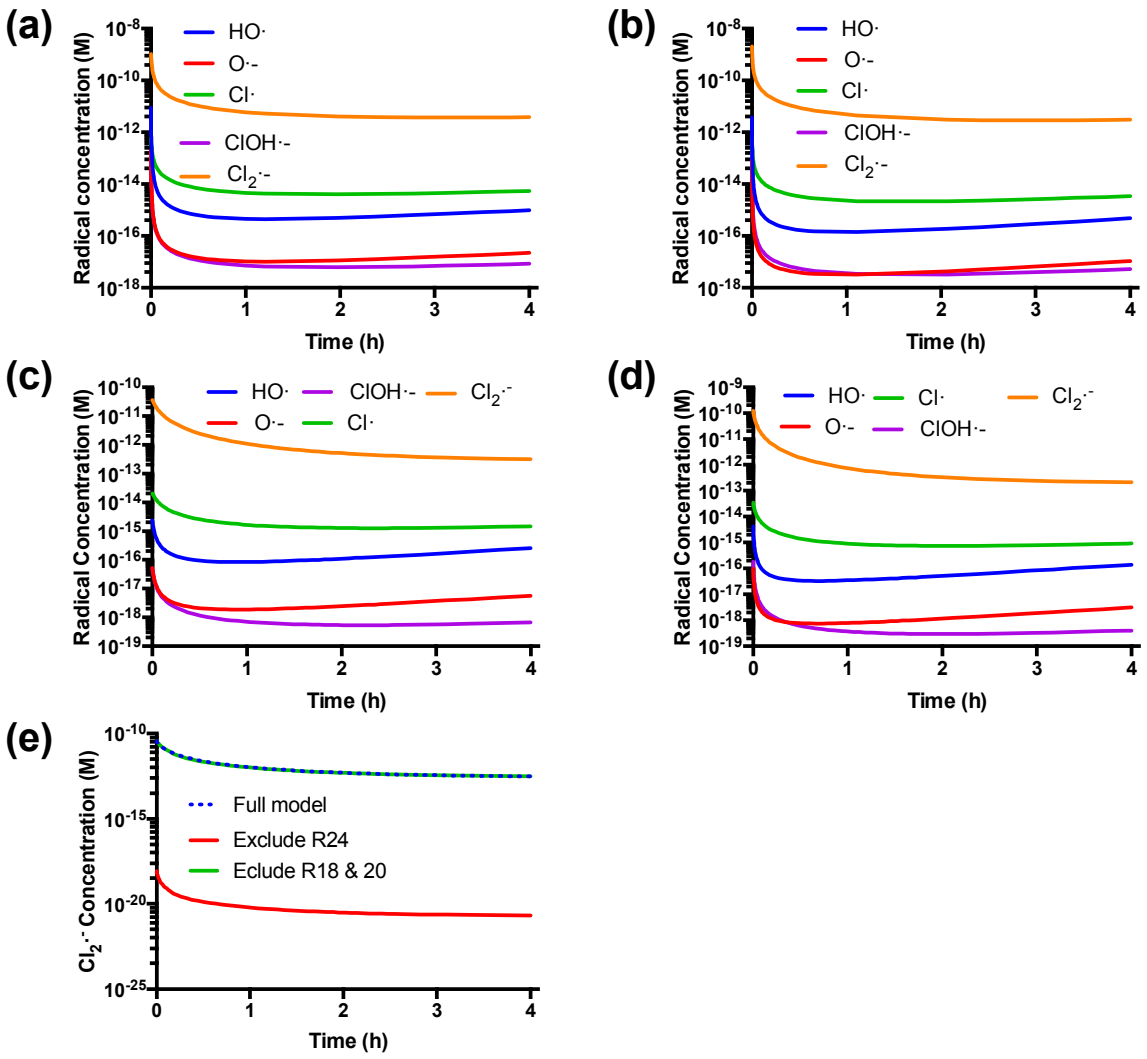

Figure S6. Model simulated radical concentration in BA degradation on SbSn/CoTi/Ir* anode operated under 25 mA/cm^2 at (a) 30 and (b) 60 mM NaCl. Model simulated radical concentration in BA degradation on SbSn/CoTi/Ir anode operated under 50 mA/cm^2 at (c) 30 and (d) 60 mM NaCl. (e) Effect of different reaction pathways on $Cl_2\cdot^-$ formation on the SbSn/CoTi/Ir anode operated at 50 mA/cm^2 in 30 mM NaCl. Excluding R18 and 20 from model (Table S2) barely affects the $Cl_2\cdot^-$ equilibrium concentration while excluding R24 significantly reduces the concentration, indicating that the combination of Cl· and Cl^- is the main pathway for $Cl_2\cdot^-$ formation.

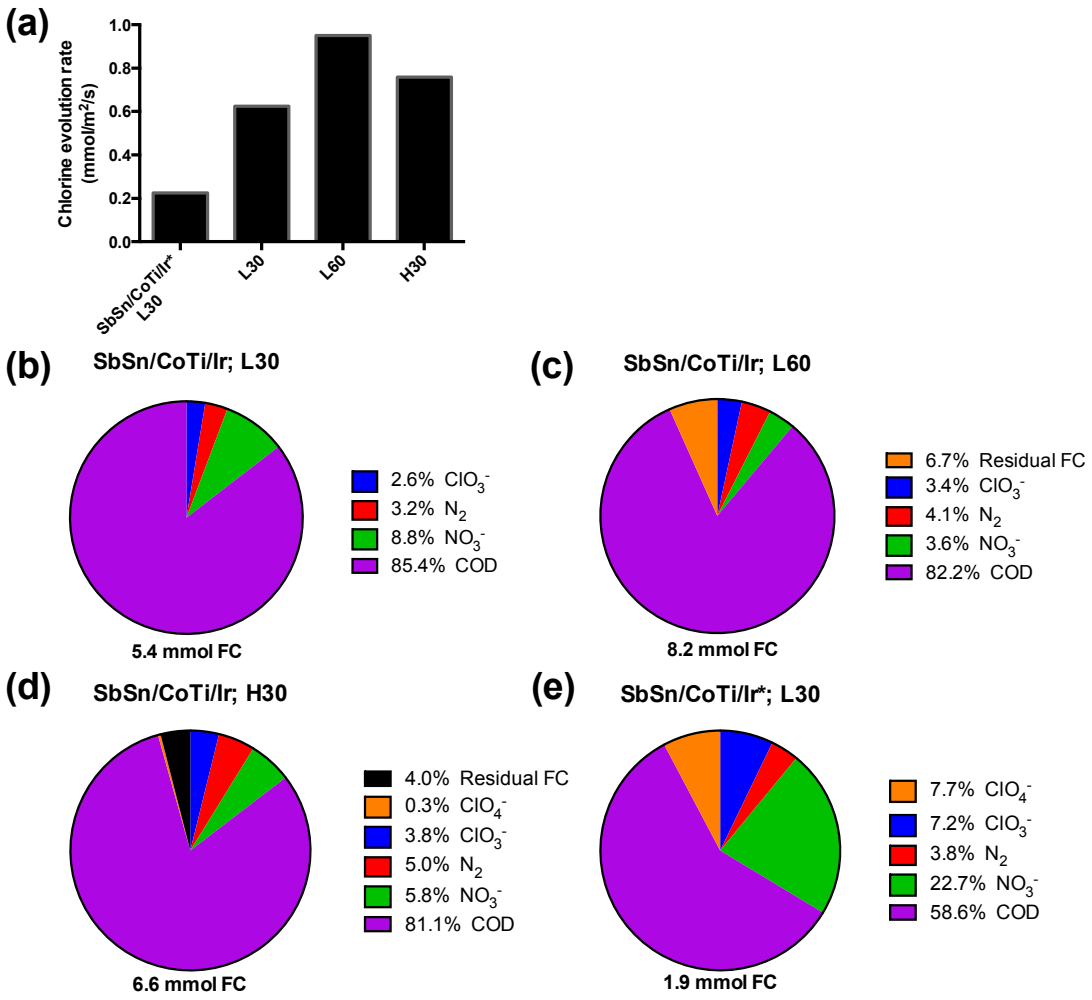

Figure S7. (a) Chlorine evolution rate of an anode operated in various modes in a NaCl electrolyte. Fate of reactive chlorine generated by SnSb/CoTi/Ir anode during human wastewater electrolysis operated in (b) L30, (c) L60, and (d) H30 modes. (e) Fate of reactive chlorine generated by SnSb/CoTi/Ir* anode during human wastewater electrolysis operated in L30 mode.

Text S1 Contribution of FC to the removal of pollutants

Figure S7a shows the chlorine evolution rate during the electrolysis of NaCl electrolyte operated in various modes. Assuming that the chlorine evolution rate would be the same in human wastewater electrolysis. Total FC generated over 4h of electrolysis can be calculated as follow:

$$FC_{total} = r_{FC} \times A \times V \times t \quad (1)$$

where r_{FC} is chlorine evolution rate, A is electrode area (6 cm^2), V is electrolyte volume (25 mL), t (s) is electrolysis duration. Operating the SbSn/CoTi/Ir anode in L30, L60, and H30 modes could produce 5.4, 8.2, and 6.6 mmol FC. While that for SbSn/CoTi/Ir* anode was 1.9 mmol.

FC could oxidize NH_3 to N_2 and NO_3^-. FC could also be converted to ClO_3^- or ClO_4^-. By subtracting the amounts of FC consumed by these reactions with well-known stoichiometries, the available FC for COD degradation (FC_{COD}, mmol) can be determined:

$$FC_{COD} = FC_{total} - \sum n_i \times \left| C_i^0 - C_i^t \right| \times V - FC_{residual} \quad (2)$$

where C_i^0 and C_i^t are the concentrations of species *i* at the electrolysis time of zero and t (s), n_i is the mole of FC required to oxidize one mole of species *i*; 1 for the oxidation of FC to ClO_3^- or ClO_4^-, 1.5 for the oxidation of NH_3 to N_2, 4 for the oxidation of NH_4^+ to NO_3^-. $FC_{residual}$ is the residual FC accumulated after breakpoint chlorination was achieved on SbSn/CoTi/Ir operated in L60 and H30 modes,

Figure S7b to e illustrate the contributions of FC to the removal of different pollutants. It could be observed that most of FC was consumed by COD degradation. For example, SbSn/CoTi/Ir anodes operated in L30 mode (Figure S7b) oxidized 0.142 mmol FC to ClO_3^-, and oxidized 0.112 mmol and 0.119 mmol of NH_3 to N_2 and NO_3^-, respectively. According to eqn (2), 4.6 mmol FC was available for COD degradation. Knowing that the removal of 0.152 mmol COD was completely contributed by FC as no radical were measured in L30 mode, the capacity of FC to oxidize COD could be expressed as a ratio of removed COD and FC_{COD}:

$$COD/FC = [COD^0 - COD^t]/FC_{COD} \quad (3)$$

which is 0.033 for L30 mode. Calculation conducted on L60 mode (Figure S7c) gave the similar value of COD/FC ratio as 0.028.

For the reaction catalyzed by SbSn/CoTi/Ir anode in H30 mode (Figure S7d), both radical pathways and FC pathways contributed to COD removal. The COD removed by FC was estimated as 0.175 mmol, by multiplying FC_{COD} (5.3 mmol) with COD/FC ratio (0.033). Given that in total 0.188 mmol COD was removed, it can be concluded that 94% of COD removal was contributed by FC, while the rest 6% was contributed by radical oxidation.

In the case of the reaction catalyzed at SbSn/CoTi/Ir* anode operated in the L30 mode, less FC was generated due to low chlorine evolution rate. Calculation showed that FC only accounted for 20% of COD removal while radical oxidation contributed 80%.

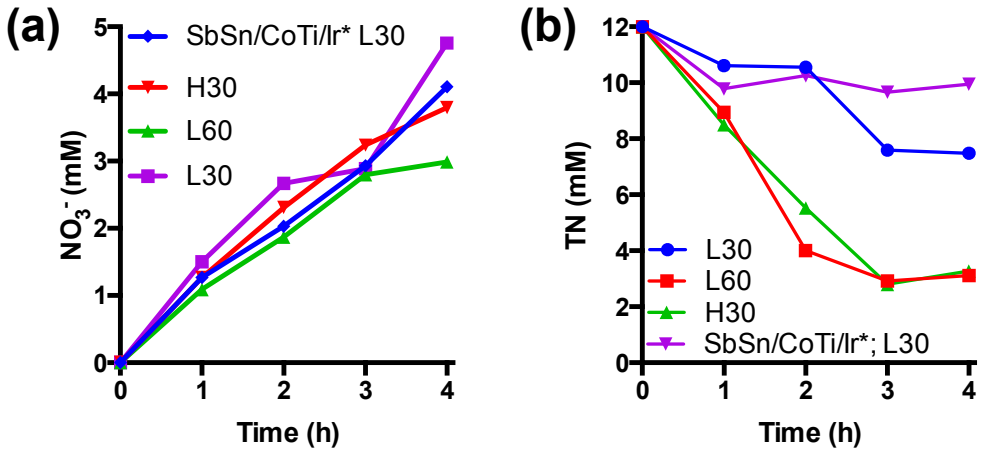

Figure S8. Time profiles of (a) NO_3^- formation and (b) total nitrogen removal on SbSn/CoTi/Ir and SbSn/CoTi/Ir* anodes under various current density (L: 25, H: 50 mA/cm^2) and initial Cl^- concentration (30, 60 mM).

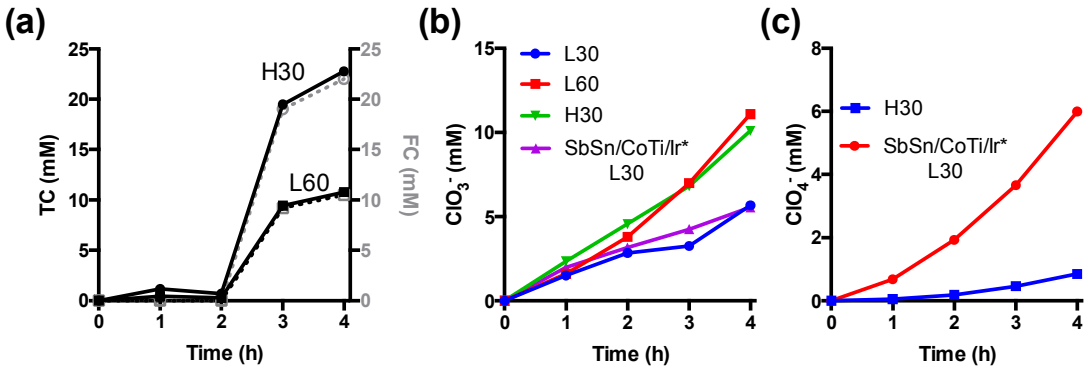

Figure S9. Time profiles of (a) the evolution of total chlorine and the formation of (b) ClO_3^- and (c) ClO_4^- on SbSn/CoTi/Ir and SbSn/CoTi/Ir* anodes under various current density (L: 25, H: 50 mA/cm^2) and initial Cl^- concentration (30, 60 mM).

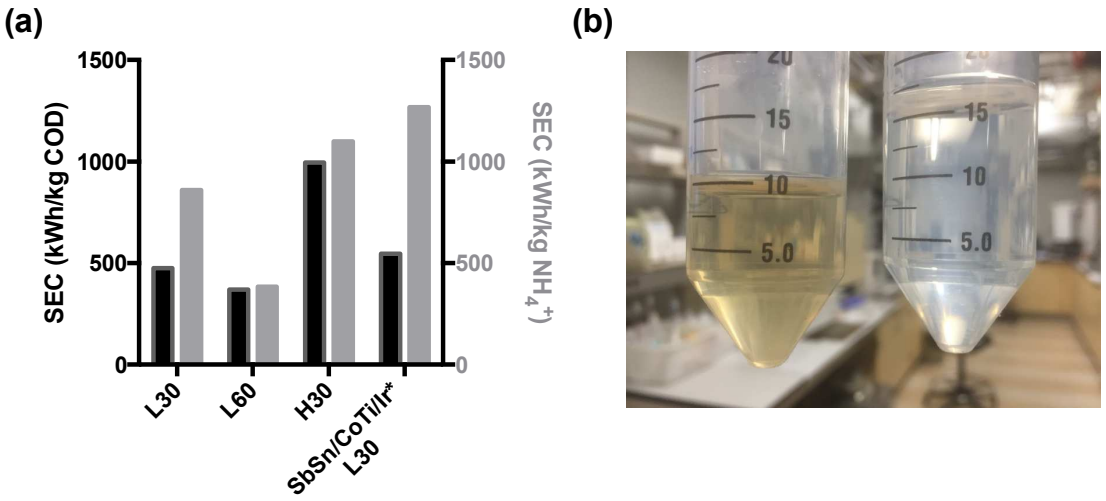

Figure S10. (a) Specific energy consumption of SbSn/CoTi/Ir and SbSn/CoTi/Ir* anodes within the initial 2 h under various current density (L: 25, H: 50 mA/cm^2) and initial Cl^- concentration (30, 60 mM). (b) Color variation of human wastewater after 4 h electrolysis under L60 condition.

Table S1. Composition of human wastewater

Composition	Mean	COV (%)
Conductivity (mS/cm)	3.2	
pH	8.5-8.8	
COD (mg/L)	240	4.7
TIC (mg/L)	312	4.5
TOC (mg/L)	73	9.7
NH_4^+ (mM)	11.98	5.4
Cl^- (mM)	29.88	9.5
PO_4^{3-} (mM)	0.56	7.6
Mg^{2+} (mM)	0.28	7.7
Ca^{2+} (mM)	0.59	4.8

Table S2. Key reactions in Na_2SO_4 and NaCl electrolysis system

Rxn No.	Reaction	Rate constant	Reference
	Composite reactions		
1[a]	$MO_x + H_2O \rightarrow MO_x + HO\cdot + H^+ + e^-$	$r_{HO\cdot}$	
2	$MO_x + Cl^- \rightarrow MO_x + Cl\cdot + e^-$	$k_{Cl\cdot}$	
3	$2MO_x + 2Cl^- \rightarrow 2MO_x + Cl_2$	k_1	
4	$MO_x + OCl^- \rightarrow MO_{x-1} + ClO_3^-$	k_2	
5	$MO_x + ClO_3^- \rightarrow MO_{x-1} + ClO_4^-$	k_3	
	pH dependent equilibrium		
6[b]	$H^+ + OH^- \rightarrow H_2O$	$1.00 \times 10^{11}\ M^{-1}\ s^{-1}$	4
7	$H_2O \rightarrow H^+ + OH^-$	$1.00 \times 10^{-3}\ M^{-1}\ s^{-1}$	4
8	$OCl^- + H^+ \rightarrow HOCl$	$5.00 \times 10^{10}\ M^{-1}\ s^{-1}$	4
9	$HOCl \rightarrow OCl^- + H^+$	$1.60 \times 10^{3}\ s^{-1}$	4
10	$Cl_2 + H_2O \rightarrow Cl_2OH^- + H^+$	$1.50 \times 10^{1}\ M^{-1}\ s^{-1}$	5
11	$Cl^- + HOCl \rightarrow Cl_2OH^-$	$1.5 \times 10^{4}\ M^{-1}\ s^{-1}$	5
12	$Cl_2OH^- \rightarrow HOCl + Cl^-$	$5.50 \times 10^{9}\ M^{-1}\ s^{-1}$	5
13	$C_6H_5COOH \Leftrightarrow C_6H_5COO^- + H^+$	$pK_a = 4.2$	6
	HO· transformation		
14	$HO\cdot + HO\cdot \rightarrow H_2O_2$	$5.50 \times 10^{9}\ M^{-1}\ s^{-1}$	7
15	$HO\cdot \rightarrow O\cdot^- + H^+$	$1.26 \times 10^{12}\ M^{-1}\ s^{-1}$	8
16	$O\cdot^- + H_2O \rightarrow HO\cdot + OH^-$	$1.80 \times 10^{6}\ M^{-1}\ s^{-1}$	8
17	$HO\cdot + OH^- \rightarrow O\cdot^- + H_2O$	$1.30 \times 10^{10}\ M^{-1}\ s^{-1}$	8
	Cl· transformation		
18	$Cl^- + HO\cdot \rightarrow ClOH\cdot^-$	$4.30 \times 10^{9}\ M^{-1}\ s^{-1}$	7
19	$ClOH\cdot^- \rightarrow Cl^- + HO\cdot$	$6.10 \times 10^{9}\ s^{-1}$	9
20	$Cl\cdot + OH^- \rightarrow ClOH\cdot^-$	$1.80 \times 10^{10}\ M^{-1}\ s^{-1}$	10
21	$ClOH\cdot^- + H^+ \rightarrow Cl\cdot + H_2O$	$2.10 \times 10^{10}\ M^{-1}\ s^{-1}$	9
22	$ClOH\cdot^- + Cl^- \rightarrow Cl_2\cdot^- + OH^-$	$1.00 \times 10^{5}\ M^{-1}\ s^{-1}$	11
23	$Cl_2\cdot^- + OH^- \rightarrow ClOH\cdot^- + Cl^-$	$4.50 \times 10^{7}\ M^{-1}\ s^{-1}$	11
24	$Cl\cdot + Cl^- \rightarrow Cl_2\cdot^-$	$6.50 \times 10^{9}\ M^{-1}\ s^{-1}$	10
25	$Cl_2\cdot^- \rightarrow Cl\cdot + Cl^-$	$1.10 \times 10^{5}\ M^{-1}\ s^{-1}$	9

26	$Cl\cdot + Cl\cdot \rightarrow Cl_2$	$1.00 \times 10^8\ M^{-1}\ s^{-1}$	12
27	$Cl\cdot + Cl_2\cdot^- \rightarrow Cl^- + Cl_2$	$1.4 \times 10^9\ M^{-1}\ s^{-1}$	13
28	$Cl_2\cdot^- + Cl_2\cdot^- \rightarrow 2Cl^- + Cl_2$	$8.30 \times 10^8\ M^{-1}\ s^{-1}$	7
29	$Cl_2\cdot^- + HO\cdot \rightarrow HOCl + Cl^-$	$1.00 \times 10^9\ M^{-1}\ s^{-1}$	7
	Radicals quenched by free chlorine		
30	$HO\cdot + HOCl \rightarrow ClO\cdot + H2O$	$2.00 \times 10^9\ M^{-1}\ s^{-1}$	4
31	$HO\cdot + OCl\text{-} \rightarrow ClO\cdot + OH^-$	$8.80 \times 10^9\ M^{-1}\ s^{-1}$	14
32	$Cl\cdot + HOCl \rightarrow ClO\cdot + H^+ + Cl^-$	$3.00 \times 10^9\ M^{-1}\ s^{-1}$	15
33	$Cl\cdot + OCl^- \rightarrow ClO\cdot + Cl^-$	$8.20 \times 10^9\ M^{-1}\ s^{-1}$	9
	Radicals quenched by benzoic acid		
34	$HO\cdot + C_6H_5COO^- \rightarrow$ Product 1	$5.90 \times 10^9\ M^{-1}\ s^{-1}$	8
35	$Cl\cdot + C_6H_5COO^- \rightarrow$ Product 2	$1.80 \times 10^{10}\ M^{-1}\ s^{-1}$	16
36	$Cl_2\cdot^- + C_6H_5COO^- \rightarrow$ Product 3	$2.00 \times 10^6\ M^{-1}\ s^{-1}$	17
37	$O\cdot^- + C_6H_5COO^- \rightarrow$ Product 4	$4.00 \times 10^7\ M^{-1}\ s^{-1}$	8

[a] Concentrations of active sites MO_x and H_2O were set as unity.

[b] Concentrations of H^+ and OH^- was set as 3.16×10^{-9} and 3.16×10^{-6}, respectively.

References

1. McCrory, C. C.; Jung, S.; Peters, J. C.; Jaramillo, T. F. Benchmarking Heterogeneous Electrocatalysts for the Oxygen Evolution Reaction. *J. Am. Chem. Soc.* **2013**, *135* (45), 16977-16987.
2. Cho, K.; Hoffmann, M. R. BixTi1-xOz Functionalized Heterojunction Anode with an Enhanced Reactive Chlorine Generation Efficiency in Dilute Aqueous Solutions. *Chem. Mater.* **2015**, *27* (6), 2224-2233.
3. Chen, X.; Chen, G.; Yue, P. L. Stable Ti/IrO_x-Sb_2O_5-SnO_2 Anode for O_2 Evolution with Low Ir Content. *J. Phys. Chem. B* **2001**, *105* (20), 4623-4628.

4. Matthew, B.; Anastasio, C. A Chemical Probe Technique for the Determination of Reactive Halogen Species in Aqueous Solution: Part 1-Bromide Solutions. *Atmos. Chem. Phys.* **2006**, *6* (9), 2423-2437.
5. Wang, T. X.; Margerum, D. W. Kinetics of Reversible Chlorine Hydrolysis: Temperature Dependence and General-Acid/Base-Assisted Mechanisms. *Inorg. Chem.* **1994**, *33* (6), 1050-1055.
6. Tao, L.; Han, J.; Tao, F.-M. Correlations and Predictions of Carboxylic Acid pKa Values Using Intermolecular Structure and Properties of Hydrogen-Bonded Complexes. *J. Phys. Chem. A* **2008**, *112* (4), 775-782.
7. NIST Standard Reference Database 40. http://kinetics.nist.gov/solution/ (accessed December 1, 2015).
8. Buxton, G. V.; Greenstock, C. L.; Helman, W. P.; Ross, A. B. Critical Review of Rate Constants for Reactions of Hydrated Electrons, Hydrogen Atoms and Hydroxyl Radicals (□OH/□O^-) in Aqueous Solution. *J. Phys. Chem. Ref. Data* **1988**, *17* (2), 513-886.
9. Jayson, G.; Parsons, B.; Swallow, A. J. Some Simple, Highly Reactive, Inorganic Chlorine Derivatives in Aqueous Solution. Their Formation Using Pulses of Radiation and Their Role in the Mechanism of the Fricke Dosimeter. *J. Chem. Soc., Faraday Trans. 1* **1973**, *69*, 1597-1607.
10. Kläning, U. K.; Wolff, T. Laser Flash Photolysis of HClO, ClO^-, HBrO, and BrO^- in Aqueous Solution. Reactions of Cl□ and Br^- Atoms. *Beri. Bunsenges. Phys. Chem.* **1985**, *89* (3), 243-245.
11. Grebel, J. E.; Pignatello, J. J.; Mitch, W. A. Effect of Halide Ions and Carbonates on Organic Contaminant Degradation by Hydroxyl Radical-Based Advanced Oxidation Processes in Saline Waters. *Environ. Sci. Technol* **2010**, *44* (17), 6822-6828.

12. Wu, D.; Wong, D.; Di Bartolo, B. Evolution of Cl2- in Aqueous NaCl Solutions. *J. Photochem.* **1980**, *14* (4), 303-310.

13. Park, H.; Vecitis, C. D.; Hoffmann, M. R. Electrochemical Water Splitting Coupled with Organic Compound Oxidation: The role of Active Chlorine Species. *J. Phys. Chem. B* **2009**, *113* (18), 7935-7945.

14. Connick, R. E. The Interaction of Hydrogen Peroxide and Hypochlorous Acid in Acidic Solutions Containing Chloride Ion. *J. Am. Chem. Soc.* **1947**, *69* (6), 1509-1514.

15. Zehavi, D.; Rabani, J. Oxidation of Aqueous Bromide Ions by Hydroxyl Radicals. Pulse Radiolytic Investigation. *J. Phys. Chem. A* **1972**, *76* (3), 312-319.

16. Mártire, D. O.; Rosso, J. A.; Bertolotti, S.; Le Roux, G. C.; Braun, A. M.; Gonzalez, M. C. Kinetic Study of the Reactions of Chlorine Atoms and Cl_2^- Radical Anions in Aqueous Solutions. II. Toluene, Benzoic Acid, and Chlorobenzene. *J. Phys. Chem. A* **2001**, *105* (22), 5385-5392.

17. Hasegawa, K.; Neta, P. Rate Constants and Mechanisms of Reaction of Chloride (Cl_2^-) Radicals. *J. Phys. Chem.* **1978**, *82* (8), 854-857.